



Effects of CO₂ perturbation on phosphorus pool sizes and uptake in a mesocosm experiment during a low productive summer season in the northern Baltic Sea

Monika Nausch¹, Lennart Thomas Bach², Jan Czerny², Josephine Goldstein^{1,a}, Hans-Peter Grossart^{4,5}, Dana Hellemann^{2,b}, Thomas Hornick⁴, Eric Pieter Achterberg^{2,3}, Kai-Georg Schulz^{2,c}, and Ulf Riebesell²

¹Leibniz Institute for Baltic Sea Research, Seestrasse 15, 18119 Rostock, Germany

²GEOMAR Helmholtz Centre for Ocean Research Kiel, Düsternbrooker Weg 20, 24105 Kiel, Germany

³Ocean and Earth Science, University of Southampton National Oceanography Centre Southampton, Southampton SO14 3ZH, UK

⁴Leibniz-Institute for Freshwater Ecology and Inland Fisheries, Zur alten Fischerhütte 2, 16775 Stechlin, Germany

⁵Potsdam University, Institute for Biochemistry and Biology, Maulbeerallee 2, 14469 Potsdam, Germany

^anow at: Max-Planck Odense Center on the Biodemography of Aging & Department of Biology, Campusvej 55, 5230 Odense M, Denmark

^bnow at: Department of Environmental Sciences, University of Helsinki, PL 65 00014 Helsinki, Finland

^cnow at: Centre for Coastal Biogeochemistry, School of Environment, Science and Engineering, Southern Cross University, Lismore, Australia

Correspondence to: Monika Nausch (monika.nausch@io-warnemuende.de)

Received: 25 September 2015 – Published in Biogeosciences Discuss.: 30 October 2015

Revised: 12 April 2016 – Accepted: 25 April 2016 – Published: 24 May 2016

Abstract. Studies investigating the effect of increasing CO₂ levels on the phosphorus cycle in natural waters are lacking although phosphorus often controls phytoplankton development in many aquatic systems. The aim of our study was to analyse effects of elevated CO₂ levels on phosphorus pool sizes and uptake. The phosphorus dynamic was followed in a CO₂-manipulation mesocosm experiment in the Storfjärden (western Gulf of Finland, Baltic Sea) in summer 2012 and was also studied in the surrounding fjord water. In all mesocosms as well as in surface waters of Storfjärden, dissolved organic phosphorus (DOP) concentrations of 0.26 ± 0.03 and $0.23 \pm 0.04 \mu\text{mol L}^{-1}$, respectively, formed the main fraction of the total P-pool (TP), whereas phosphate (PO₄) constituted the lowest fraction with mean concentration of 0.15 ± 0.02 in the mesocosms and $0.17 \pm 0.07 \mu\text{mol L}^{-1}$ in the fjord. Transformation of PO₄ into DOP appeared to be the main pathway of PO₄ turnover. About 82 % of PO₄ was converted into DOP whereby only 18 % of PO₄ was transformed into particulate phosphorus (PP). PO₄ uptake rates measured in the mesocosms ranged between 0.6 and $3.9 \text{ nmol L}^{-1} \text{ h}^{-1}$. About 86 % of them was

realized by the size fraction $< 3 \mu\text{m}$. Adenosine triphosphate (ATP) uptake revealed that additional P was supplied from organic compounds accounting for 25–27 % of P provided by PO₄ only. CO₂ additions did not cause significant changes in phosphorus (P) pool sizes, DOP composition, and uptake of PO₄ and ATP when the whole study period was taken into account. However, significant short-term effects were observed for PO₄ and PP pool sizes in CO₂ treatments $> 1000 \mu\text{atm}$ during periods when phytoplankton biomass increased. In addition, we found significant relationships (e.g., between PP and Chl *a*) in the untreated mesocosms which were not observed under high *f*CO₂ conditions. Consequently, it can be hypothesized that the relationship between PP formation and phytoplankton growth changed with CO₂ elevation. It can be deduced from the results, that visible effects of CO₂ on P pools are coupled to phytoplankton growth when the transformation of PO₄ into POP was stimulated. The transformation of PO₄ into DOP on the other hand does not seem to be affected. Additionally, there were some indications that cellular mechanisms of P regulation might be modified un-

der CO₂ elevation changing the relationship between cellular constituents.

1 Introduction

Increasing emissions of anthropogenic CO₂ into the atmosphere and subsequent acidification of the ocean can potentially affect the diversity of organisms and the functioning of marine ecosystems (Eisler, 2012). The rise in atmospheric CO₂ concentrations was accelerated from 3.4 ± 0.2 in the 1980s to 4.0 ± 0.2 PgC yr⁻¹ in the 2000s leading to increases of CO₂ in ocean surface waters at a similar rate (IPCC, 2013). Atmospheric CO₂ is projected to rise to 750–1000 ppm and higher in 2100 (IPCC, 2001) corresponding with a decrease in open ocean pH by 0.3–0.5 units (Caldeira and Wickett, 2005) from the present level of ~ 8.1 . Although this process is of global significance and all parts of the oceans are at risk, there will be regional differences in the degree of acidification (Borges et al., 2005). Thus, to determine the CO₂-related changes in the oceans, multiple studies in different regions are required. Semi-enclosed coastal regions, such as the Baltic Sea, react with higher changes in pH to CO₂ elevation than open ocean waters due to high freshwater inputs resulting in a reduced buffer capacity (Orr, 2011).

In the Baltic Sea, several studies of CO₂ effects have been undertaken on the organism level of fish (Frommel et al., 2013), zooplankton (Pansch et al., 2012; Vehmaa et al., 2012), macrophytes (Pajusalu et al., 2013), benthic species (Hiebenthal et al., 2013; Stemmer et al., 2013), and filamentous cyanobacteria (Czerny et al., 2009; Eichner et al., 2014; Wannicke et al., 2012). Studies on the impacts of elevated CO₂ at the ecosystem level, however, have thus far been limited to Kiel Bight in the western Baltic Sea (Engel et al., 2014; Rossoll et al., 2013; Schulz and Riebesell, 2013), which may fundamentally differ from other parts of the Baltic Sea.

Next to nitrogen, phosphorus (P) controls the productivity of phytoplankton in the ocean (Karl, 2000; Sanudo-Wilhelmy et al., 2001; Tyrrell, 1999) and is a limiting factor in some regions (Ammerman et al., 2003). The total phosphorus (TP) pool comprises phosphate (PO₄), dissolved organic phosphorus (DOP), and particulate organic (POP) and inorganic (PIP) phosphorus. There is a continuous transformation of phosphorus between these P species due to their uptake, conversion, and release by organisms as well as by interaction with minerals. While PO₄ is the preferred P-species of phyto- and bacterioplankton, DOP can become an important P source when PO₄ is depleted (Llebot et al., 2010; Lomas et al., 2010). DOP includes nucleic acids, phospholipids, and adenosine triphosphate (ATP; Karl and Björkman, 2002) which are structural and functional components of all living cells, but, can also be released into the surrounding water.

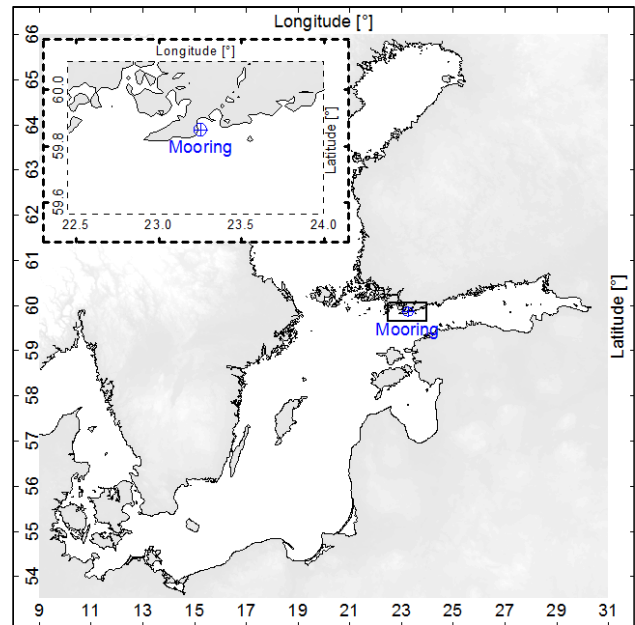


Figure 1. The Baltic Sea and the location near the peninsula Hanko in the western Gulf of Finland where the mesocosms were deployed.

In general, there is little knowledge on how the P cycle is affected by ocean acidification and how related changes in P availability influence the response of organisms to CO₂ elevation. In CO₂ manipulation experiments, particulate phosphorus dynamics were studied to determine effects on C:P stoichiometry of phytoplankton (Riebesell and Tortell, 2011; Sugie and Yoshimura, 2013) and PO₄ concentration dynamics to estimate its utilization (Bellerby et al., 2008). CO₂ effects on phosphorus pool sizes and PO₄ uptake have so far been studied by Tanaka et al. (2008) in the Raunefjorden, Norway and by Unger et al. (2013) and Endres et al. (2013) in laboratory experiments with cultures of *Nodularia spumigena*. In order to reduce the gap of knowledge, we studied the impact of elevated CO₂ on phosphorus pool sizes, the DOP composition, and PO₄ uptake of a northern Baltic Sea plankton community. These measurements provide important information on potential changes in P cycling under increasing CO₂ levels and contribute to a better understanding of the P cycle in brackish water ecosystems.

2 Material and methods

2.1 Experimental design and CO₂ manipulation

The study was conducted in the northwestern Gulf of Finland, in the proximity of the Tvärminne Zoological Station (TZS; Fig. 1), between 17 June and 4 August 2012, using the KOSMOS mesocosm system (Riebesell et al., 2013). Nine mesocosms (M1–M9) were moored in the open waters of the Storfjärden (5951.5° N, 2315.5° E) at a water depth

of ~ 30 m. Only six of them were included throughout the whole study period since leakages in the remaining three rendered them unusable. Equipment and deployment procedures are described in detail by Paul et al. (2015b). Briefly, polyurethane enclosure bags of 2 m in diameter and 18.5 m in length were mounted in floating frames and lowered in such a way that ~ 17 m of each bag was immersed in the water column and ~ 1.5 m remained above the water surface. Large organisms were excluded from the mesocosms by a 3 mm mesh installed at the top and bottom of the bags before closure. The mesocosms were deployed 10 days prior to CO₂ manipulation to rinse the bags and for full water exchange. Sediment traps were mounted on the lower ends to close them water tight, while the upper ends were raised above the water surface to prevent water entry during wave action. The mesocosms were covered with a dome-shaped roof to prevent nutrient input by birds and potentially significant fresh water input by rain. Salinity gradients were removed by bubbling the mesocosms with compressed air for 3.5 min, so that 5 days before the start of the experiment (day -5) the water body was fully homogeneous.

CO₂ was injected at day 0 and the subsequent 4 days by pumping various quantities of 50 µm-filtered and CO₂-enriched fjord water into seven of the mesocosms as described by Riebesell et al. (2013). The intended CO₂ and pH gradients were reached after the last treatment on day 4. Details are described in Paul et al. (2015b). For the two untreated (control) mesocosms, only filtered fjord water was added to adjust the water volume to that of the treated mesocosms. To compensate for outgassing, the CO₂ manipulation was similarly repeated in the upper 7 m layer of the mesocosms on day 16.

2.2 Sampling

Daily sample collection started 3 days before the first CO₂ injection (day -3). Parallel samples were taken from the surrounding fjord. Sampling over the entire 17 m depth was carried out using an integrating water sampler (IWS HYDROBIOS-KIEL) that was lowered slowly on a cable by hand. The sampling frequency differed depending on the parameter to be observed as shown in the overview by Paul et al. (2015b).

Phosphorus pool parameters and uptake rates were determined every second day, except for dissolved organic phosphorus (DOP) components, which were measured every 4 days. Termination of the measurements varied due to logistical constraints. Thus, total phosphorus (TP) and DOP were sampled only until day 29 whereas other parameters were sampled until day 43.

The collected water was filled in HCl-cleaned polyethylene canisters that had been pre-rinsed with sample water. All containers were stored in the dark. Back on land, subsamples were processed immediately for each P-analysis. The other analyses were carried out within a few hours of sample col-

lection and sample storage in a climate room at in situ temperature.

2.3 Analytical methods

2.3.1 Temperature, salinity, and carbonate chemistry

Measurements in the fjord and in each mesocosm were conducted using a CTD60M memory probe (Sea and sun technology, Trappenkamp, Germany) lowered from the surface to a depth of 17 m at about 0.3 m s⁻¹ in the early afternoon (01:30–02:30 p.m.). For these parameters, depth-integrated mean values are presented here.

The carbonate system is described in detail in Paul et al. (2015b). The pHT (total scale) was determined using a spectrophotometric method (Dickson et al., 2007) on a Cary 100 (Varian) and the dye m-cresol as indicator. Extinction was measured at 578 (E1) and 434 nm (E2) in a 10 cm cuvette. The pH was calculated from the ratio of E1 and E2 (Clayton and Byrne, 1993).

DIC was measured using a coulometric AIRICA system (MARIANDA, Kiel) measuring the infrared absorption after N₂ purging of the sample and calibration with certified reference material (CRM; A. Dickson, University of California, San Diego).

The *f*CO₂ was calculated from DIC, pHT, salinity and using the stoichiometric equilibrium constant for carbonic acid of Mehrbach et al. (1973) as refitted by Lueker et al. (2000).

2.3.2 Chlorophyll and inorganic nutrients

Subsamples of 500 mL were filtered onto GF/F-filters. Chl *a* was extracted in acetone (90 %) in plastic vials by homogenisation of the filters for 5 min in a cell mill using glass beads. After centrifugation (10 min, 800 × *g*, 4 °C) the supernatant was analysed on a fluorometer (TURNER 10-AU) at an excitation of 450 nm and an emission of 670 nm to determine Chl *a* concentrations (Jeffrey and Welschmeyer, 1997).

A segmented continuous-flow analyzer coupled with a liquid-waveguide capillary flow-cell (LWCC) of 2 m length was used to determine phosphate (PO₄) and the sum of nitrite and nitrate (NO₂ + NO₃) at nanomolar precision (Patey et al., 2008). The PO₄ determination was based on the molybdenum blue method of Murphy and Riley (1962), and NO₃+NO₂ on the method of Morris and Riley (1963). PO₄ concentrations from the same subsample were also measured manually using a 5 cm cuvette (Grasshoff et al., 1983). In most of the samplings PO₄ data obtained from both methods did not differ significantly (paired *t* test: *p* = 0.262, *t* = 1.127, *n* = 109).

2.3.3 Dissolved organic phosphorus (DOP)

For the determination of DOP, duplicate 40 mL subsamples were filtered through pre-combusted (6 h, 450 °C) glass fiber filters (Whatman GF/F) and stored in 50 mL vials (Falcon) at

–20 °C until further processing. The thawed samples were oxidized in a microwave (MARSXpress, CEM, Matthews, USA; Johns and Heathwaite, 1992) after the addition of potassium peroxydisulfate in an alkaline medium (Bhaya et al., 2000). The P concentration, measured as PO₄ in a 10 cm cuvette, represents the total dissolved phosphorus (DP) concentration. DOP was calculated as the difference between the DP concentrations in the filtered and digested samples and the corresponding PO₄ concentration analysed as described above.

2.3.4 Dissolved organic phosphorus compounds

For all analysed components, subsamples were pre-filtered through pre-combusted (6 h, 450 °C) filters (Whatman GF/F) to remove larger particles followed by filtration through 0.2 µm cellulose acetate filters to remove picoplankton. Subsamples were prepared for storage according to the specific method used for each compound. After the analyses, the phosphorus content of measured DOP compounds was summed and the amount subtracted from the total DOP concentration. The difference is defined as the uncharacterized DOP.

Dissolved ATP

The method of (Björkman and Karl, 2001) adapted to Baltic Sea conditions (Unger et al., 2013) was used to determine dissolved adenosine triphosphate (dATP). An Mg(OH)₂ precipitate, including the co-precipitated nucleotides, was obtained by treating 200 mL of the filtrate with 2 mL of 1 M NaOH (1 % *v/v*). The precipitate was allowed to settle overnight and then centrifuged at 1000 g for 15 min. The supernatant was discarded and the precipitate was transferred into 50 mL Falcon tubes, centrifuged again (1.5 h, 1680 × *g*). The resulting pellet was dissolved by drop-wise addition of 5 M HCl. The samples were frozen at –20 °C until further processing. The pH of the thawed samples was adjusted to 7.2 by the addition of TRIS buffer (pH 7.4, 20 mM). The final volume was recorded. The dATP concentrations were measured in triplicate using the firefly bioluminescence assay and a Sirius luminometer (Berthold Detection Systems Pforzheim, Germany), as described by Unger et al. (2013). Standard concentrations were prepared as described above, using aged Baltic Sea water and six ATP concentrations (adenosine 50-triphosphate disodium salt hydrate, Sigma-Aldrich, A2383) ranging from 1 to 20 nmol L^{–1}. The detection limit of the bioluminescence assay was 2.5 nmol L^{–1}. The fluorescence slope of the standard concentrations was used to calculate dATP concentrations, correcting for the final sample volume. The P-content of the dATP (dATP-P) was calculated by assuming that 1 mol of ATP is equivalent to 3 mol P.

Dissolved phospholipids

The phosphate content of the dissolved phospholipids (PL-P) was analysed using a modified method of Suzumura and In-gall (2001, 2004). Briefly, 400 mL subsamples of the filtrate were stored at –20 °C until further processing. The samples were then thawed in a water bath at 30 °C and extracted twice with 100 mL of chloroform. The chloroform phase was collected, concentrated to 5 mL in a rotary evaporator (Heidolph Instruments, Schwabach, Germany), and then transferred into microwave tubes. The chloroform was completely evaporated by incubating the tubes in a 60 °C water bath overnight. After the addition of 20 mL of deionized water (Milli-Q, Millipore), the samples were digested with potassium peroxydisulfate in alkaline medium and microwaved as described for the DOP analysis. Six standard concentrations of phospholipids, ranging from 0 to 125 µg L^{–1}, were prepared by adding the respective amounts of a stock solution containing 5 mg of 1-phosphatidyl-dl-glycerol sodium salt (PG, Sigma Aldrich, P8318) mL^{–1} to the aged seawater. The detection limit was 0.8 nmol L^{–1}. The blanks contained only chloroform and were processed as for the samples.

Dissolved DNA and RNA

Dissolved DNA and RNA (dDNA and dRNA) concentrations were determined according to Karl and Bailiff (1989) and as described by Unger et al. (2013). For each sample, 200 mL of the filtrate was gently mixed with the same volume of ethylene-diamine-tetracetic acid (EDTA, 0.1 M, pH 9.3, Merck, 1.08454) and 4 mL of cetyltrimethyl-ammonium bromide (CTAB, Sigma-Aldrich, H5882) and stored frozen at –20 °C for at least 24 h. After thawing the samples, the precipitate was collected onto combusted (450 °C, 6 h) glass fiber filters (25 mm, GF/F Whatman), placed into annealed vials, and stored frozen at –80 °C until further analysis.

DNA concentrations were measured using a fluorescence-spectrophotometer (Hitachi F 2000), and RNA concentrations using a dual-beam UV/VIS-spectrophotometer U3010 (Hitachi).

Coupled standards (DNA + RNA) containing 1–10 µg DNA (Sigma Aldrich, D3779) L^{–1} and 20–120 µg RNA (Sigma Aldrich, R1753) L^{–1} were prepared in aged seawater as described above. A reagent blank served as the reference and aged seawater as the background control. The P-contents of the DNA and RNA were calculated by multiplying the measured values by a factor of 2.06 nmol P per µg dDNA and 2.55 nmol P per µg dRNA. The latter values were determined by the microwave digestion of standard substrates.

2.3.5 Particulate organic phosphorus, carbon, and nitrogen

Particulate phosphorus (PP) was analysed using two methods in parallel. In the “aqueous method”, 40 mL of unfil-

tered subsamples were frozen at -20°C and analysed as described for DOP using the potassium peroxydisulfate digestion (Grasshoff et al., 1983). The measured PO₄ concentration represents total phosphorus (TP). PP is the difference between the TP concentration in the unfiltered digested sample and the sum of DOP+PO₄. In the “filter-method”, 500 mL subsamples were filtered onto pre-combusted GF/F filters that were then placed into Schott bottles containing 40 mL of deionised water. PP was digested to PO₄ by the addition of oxidizing decomposition reagent (Oxisolv[®], Merck) followed by heating in a pressure cooker for 30 min. The PO₄ concentrations of the cooled samples were determined spectrophotometrically according to Grasshoff et al. (1983). Paired *t* test revealed significant differences between two methods; however, the difference between the means of the filter method and of the aqueous method ($0.19 \pm 0.03 \text{ mmol L}^{-1}$ and $0.1 \pm 0.04 \text{ } \mu\text{mol L}^{-1}$, respectively) were near the detection limit ($0.02 \text{ } \mu\text{mol L}^{-1}$) of the methods. Thus, solely the mean values obtained from both measurements are used in the following.

Particulate carbon (PC) and nitrogen (PN) were analysed by filtering 500 mL samples onto pre-combusted (450°C , 6 h) glass fiber filters (Whatman GF/F), which were then stored frozen at -20°C . PC and PN concentrations were measured by flash combustion of the dried (60°C) filters using a EuroEA elemental analyser coupled with a ConFlo II interface to a Finnigan Delta^{Plus} mass spectrometer and included organic and inorganic matter.

2.3.6 Phosphate and ATP uptake

PO₄ uptake was measured by addition of radioactively labelled phosphate [³³P]PO₄ (specific activity of $111 \text{ TBq mmol}^{-1}$, Hartmann Analytic GmbH) at concentrations of 50 pmol L^{-1} to 50 mL subsamples, which were then incubated under laboratory light and the in situ temperatures for $\sim 2 \text{ h}$. For each mesocosm, three parallel samples and a blank were prepared. The blank was obtained by the addition of formaldehyde (1 % final concentration) 10 min before radiotracer addition, in order to poison the samples. At defined time intervals within the incubation, 5 mL subsamples were taken from each of the parallel samples and filtered onto polycarbonate (PC) filters pre-soaked with a cold 20 mM PO₄ solution to prevent non-specific [³³P]PO₄ binding. The filters were rinsed with 5 times 1 mL of particle-free bay water and placed in 6 mL scintillation vials. Scintillation liquid (4 mL IrgaSafe; Perkin Elmer) was added and the contents of the vials were mixed using a vortex mixer. After allowing the samples to stand for at least 2 h, the radioactivity on the filters was counted in a Perkin Elmer scintillation counter. PC-filters of 0.2 μm and 3 μm pore sizes (Whatman and Millipore, respectively) were used to determine uptake by the whole plankton community and the size fraction $> 3 \text{ } \mu\text{m}$, respectively. Picoplankton uptake was calculated as the difference between the activity on the 0.2 and 3 μm filters.

[γ ³³P]ATP (specific activity of $111 \text{ TBq mmol}^{-1}$, Hartmann Analytic GmbH) was added to triplicate 10 mL samples and a blank, each in a 20 mL vial, at a concentration of 50 pmol L^{-1} . The samples were incubated in the dark at the in situ temperature for 1 h. The uptake was stopped by addition of 200 μL of a cold 20 mM ATP solution to the samples, which were then filtered and processed as described for the PO₄ uptake measurements.

2.3.7 Bacterial production (BPP)

Rates of bacterial protein production (BPP) were determined by incorporation of [¹⁴C]-leucine (¹⁴C-Leu, Simon and Azam, 1989) according to Grossart et al. (2006). Triplicates and a formalin-killed control were incubated with ¹⁴C-Leu ($7.9 \text{ GBq mmol}^{-1}$; Hartmann Analytic GmbH, Germany) at a final concentration of 165 nmol L^{-1} , which ensured saturation of uptake systems of both free and particle-associated bacteria. Incubation was performed in the dark at in situ temperature (between 7.8 and 15.8°C) for 1.5 h. After fixation with 2 % formalin, samples were filtered onto 5.0 μm (attached) nitrocellulose filters (Sartorius, Germany) and extracted with ice-cold 5 % trichloroacetic acid (TCA) for 5 min. Thereafter, filters were rinsed twice with ice-cold 5 % TCA, once with ethanol (96 % *v/v*), and dissolved with ethylacetate for measurement by liquid scintillation counting. Afterwards the collected filtrate was filtered on 0.2 μm (free-living) nitrocellulose filters (Sartorius, Germany) and processed in the same way as the 5.0 μm filters. Standard deviation of triplicate measurements was usually $< 15 \%$. The sum of both fractions (free-living bacteria and attached bacteria) is referred to total BPP. The amount of incorporated ¹⁴C-Leu was converted into BPP by using an intracellular isotope dilution factor of 2 (Simon and Rosenstock, 1992). A conversion factor of 0.86 was used to convert the protein produced into carbon (Simon and Azam, 1989).

2.4 Statistical analyses

The Grubbs test, done online (graphpad.com/quickcalcs/Grubbs1.cfm) was applied to identify outliers in all data sets. The outliers were removed from further statistical analyses.

Spearman Rank correlations were carried out to describe the relationship between the development of the parameters over time in the mesocosms and in the fjord using Statistica 6 software.

Short-term CO₂ effects on PP concentrations at days 0–2 and 23–43 between the CO₂ treatments were verified with an ANCOVA analysis using the SPSS software. The “days” were treated as a covariate interacting with the treatments. Paired *t* test was applied to check the differences in PO₄ concentrations between the treatments.

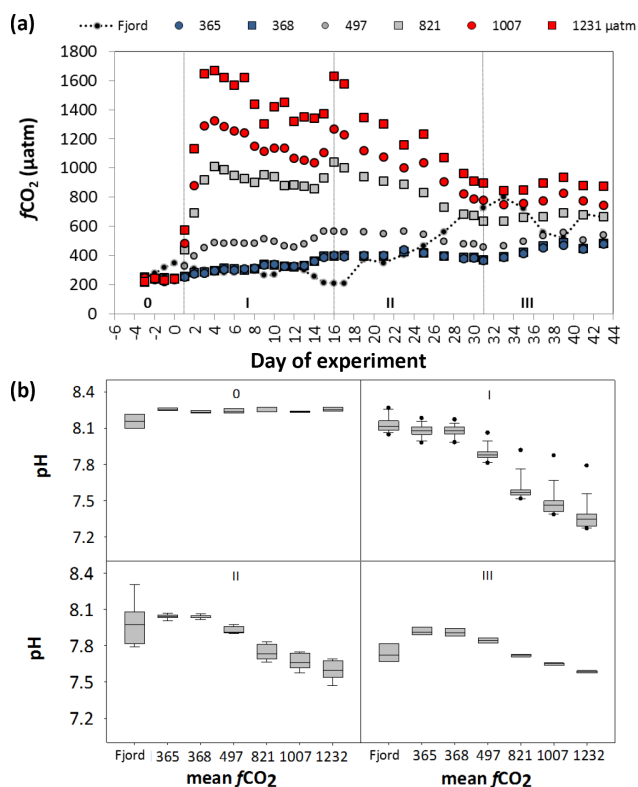


Figure 2. (a) $f\text{CO}_2$ values in the mesocosms and in the fjord throughout the experiment. Small black dots show the $f\text{CO}_2$ in the ambient fjord water. Treatment of the mesocosms with CO₂ saturated fjord water at the beginning of the experiment (days 0–4) created different $f\text{CO}_2$ levels in the mesocosms: blue symbols represent the untreated mesocosms, grey the intermediate, and red the high CO₂ treated mesocosms. The treatment was repeated at day 16. (b) Corresponding pH ranges in the mesocosms during the four phases. Despite decreasing trends over time, a gradient between the mesocosms was kept over the whole period.

3 Results

3.1 Development in the mesocosms

3.1.1 CO₂, pH, temperature and salinity

The different mesocosms were characterized based on their averaged $f\text{CO}_2$ and pH values from day 1 until day 43 (Fig. 2a, b):

- M1 365 μatm $f\text{CO}_2$, pH 8.08
- M5 368 μatm $f\text{CO}_2$, pH 8.07
- M7 497 μatm $f\text{CO}_2$, pH 7.95
- M6 821 μatm $f\text{CO}_2$, pH 7.74
- M3 1007 μatm $f\text{CO}_2$, pH 7.66
- M8 1231 μatm $f\text{CO}_2$, pH 7.58

M1 and M5 were the untreated mesocosms and served as controls.

Temperature development in the mesocosms closely followed that in the fjord ranging from 7.82 to 15.86 °C. Based

Table 1. Minimum, maximum and mean values of hydrographical parameters and $f\text{CO}_2$ for the different phases in the fjord. Temperatures in the mesocosms were identical with those in surrounding fjord water.

phase	min	max	mean
water temperature (°C)			
0	7.82	8.71	8.20
I	9.66	15.86	12.27
II	7.89	14.79	11.68
III	8.35	12.61	10.83
salinity			
0	5.72	5.85	5.78
I	5.46	5.85	5.65
II	5.67	6.04	5.82
III	5.9	6.05	5.98
pH			
0	8.09	8.23	8.16
I	8.11	8.30	8.17
II	7.81	8.30	8.00
III	7.75	7.93	7.83
$f\text{CO}_2$ (μatm)			
0	250	347	298
I	207	336	283
II	208	679	465
III	521	800	668

on this (compare Paul et al., 2015b for details), the experiment was divided into four phases (Fig. 3): phase 0: day –3 to day 0; phase I: days 1–16, phase II: days 17–30 and phase III: day 31 until the end of the measurements. Temperature dropped from 8.71 to 7.82 °C in phase 0 and rose from 8.07 °C at the start of phase I to the maximum of 15.86 °C by the end of this phase. During phase II, the temperature decreased to 7.89 °C interrupted by a short reversal on days 22 and 23. During phase III, the temperature increased to 12.61 °C (Table 1).

Salinity (5.69 ± 0.01) remained relatively stable in all mesocosms throughout the entire experimental period (Fig. 3).

3.1.2 Phytoplankton biomass

Chlorophyll *a* (Chl *a*) reached maximum concentrations of $2.06\text{--}2.48 \mu\text{g L}^{-1}$ at day 5 (Fig. 4). Average concentrations of $1.94 \pm 0.23 \mu\text{g L}^{-1}$ in phase I exceeded those in phases II and III when Chl *a* decreased to a mean of $1.08 \pm 0.16 \mu\text{g L}^{-1}$. The increase in Chl *a* in the high CO₂ mesocosms by $0.27 \mu\text{g L}^{-1}$ in phase III was marginal for Baltic Sea summer conditions. According to Paul et al. (2015b), this represents an increase of 24% which is a significant difference compared to the controls.

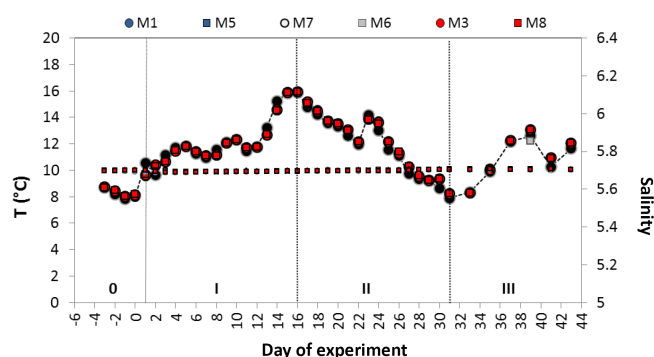


Figure 3. Temperature and salinity averaged over the 17 m surface layer of the mesocosms and the fjord. The data were obtained from daily CTD casts. Large symbols represent temperature and the small symbols salinity. Fjord water is shown as black dots with broken line while blue symbols denote untreated, grey intermediate and red high $f\text{CO}_2$ levels in the mesocosms. According to the temperature regime, the experimental period can be divided into four phases (phases 0, I, II and III).

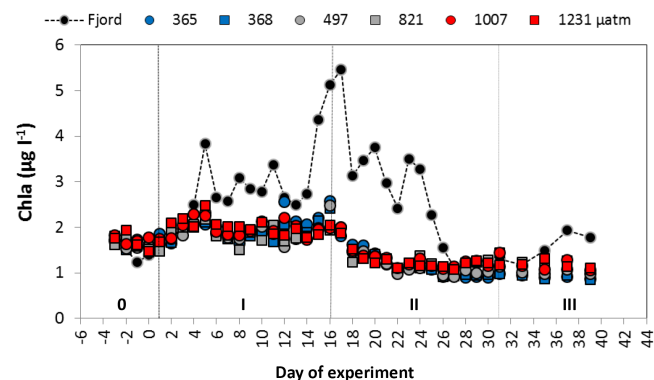


Figure 4. Chl *a* concentrations in fjord water and in the mesocosms with different $f\text{CO}_2$ conditions. The development over time can be divided into three phases as well. Blue represents untreated, grey intermediate, and red highly treated $f\text{CO}_2$ levels. Black dots with dotted line are the Chl *a* concentrations in the fjord water.

We observed a significant relationship between Chl *a* and PO_4 in the untreated and intermediate treated mesocosms that diminished with increasing $f\text{CO}_2$ as indicated by lower p values. The statistical significance was lost in the highest $f\text{CO}_2$ mesocosms (Table 2).

3.1.3 Phosphorus pools

Total phosphorus (TP) concentrations in the mesocosms ranged between 0.49 and $0.68 \mu\text{mol L}^{-1}$ (Fig. 5a) during the experiment without statistically significant differences between the CO₂ treatments. Shortly after the bags were closed, the decline in TP concentrations began and continued until the beginning of phase II. On average, TP concentrations decreased from 0.63 ± 0.02 on day -3 to $0.51 \pm 0.01 \mu\text{mol L}^{-1}$

on day 21. Thereafter, the mean TP remained constant at $0.54 \pm 0.03 \mu\text{mol L}^{-1}$ until the end of the measurements. Thus, the loss of phosphorus ($116 \pm 34 \text{ nmol L}^{-1}$) from the 17 m layer during the 29-day measurement period was calculated to be $4.0 \text{ nmol L}^{-1} \text{ day}^{-1}$. The decline in TP can be explained by loss through sedimentation of PP (Paul et al., 2015b).

Particulate phosphorus (PP) concentrations varied from 0.10 to $0.23 \mu\text{mol L}^{-1}$ in all CO₂ treatments (Figs. 5b, 6). We expected that the decrease in TP was reflected in PP. However, parallel changes occurred only periodically. PP concentrations increased during the first 5 days after the bags were closed. This increase was stimulated by CO₂ additions from day 0 to day 2 (ANCOVA: $p = 0.004$, $F = 20.811$; Fig. 7a). Subsequently, PP declined in parallel with TP until day 21, albeit with a lower amount. Averaged over all mesocosms, TP decreased by $0.12 \pm 0.03 \mu\text{mol L}^{-1}$, whereas PP declined only by $0.06 \pm 0.01 \mu\text{mol L}^{-1}$ during this period. From day 23 until the end of the measurements, PP remained at relatively constant concentrations; however, PP concentrations in the high CO₂ treated mesocosms exceeded those in the other mesocosms significantly (ANCOVA: $p < 0.0001$, $F = 11.99$; Figs. 5b, 7). PP developed in parallel with PC. The two parameters were positively correlated in the untreated and the intermediate CO₂ treatments, but not in the high CO₂ treatments (Table 2). Figures 3 and 6b show that the increase in Chl *a* was delayed by 2–3 days compared to the increase in PP during the first growth event. A correlation between PP and Chl *a* was detected only for the untreated mesocosms (Table 2).

Dissolved organic phosphorus (DOP) concentrations in the mesocosms ranged between 0.18 and $0.36 \mu\text{mol L}^{-1}$ constituting 32–71 % of the TP pool (Fig. 5c). DOP did not change significantly in response to the CO₂ perturbations, and were similar to the concentrations in fjord water. Concentrations of $\geq 0.3 \mu\text{mol L}^{-1}$ were measured on days 6 and 7 (phase I) and on day 23 (phase II); the high DOP value in the intermediate CO₂ treatment at day 19 was identified as an outlier according to Grubbs test (Fig. 5c).

In phase I, DOP initially increased in parallel with Chl *a* and BPP but reached its maximum 1–2 days later, after which it decreased only marginally until the end of this phase, independent of changes in BPP and Chl *a* (Fig. 8c, d). In phase II, the peak conformed to that of BPP. DOP correlated with temperature only in the high $f\text{CO}_2$ mesocosms (Table 2). In addition, the composition of DOP did not change with increasing CO₂ (Fig. 10). The sum of RNA ($\sim 47\%$) plus the unidentified fraction constituted 98–99 % of the DOP pool whereas the other measured compounds contributed only 1–2 % (Table 3).

Phosphate (PO_4) concentrations ranged between 0.06 and $0.21 \mu\text{mol L}^{-1}$, with deviations between the mesocosms only in nanomolar range. The mean contribution of PO_4 to TP was $25 \pm 6\%$, which was the lowest among all TP fractions (Fig. 6). From the start of the measurements to day

Table 2. Mesocosms in which the Spearman Rank correlation between P-pools or uptake rates and other parameters was significant. The relationship of PP with TP and Chl *a* was significant only in the untreated mesocosms while the correlation to PC was also significant in the mesocosms with intermediate CO₂ levels. DOP was related to temperature only in the high CO₂ treatments. Under high *f*CO₂ conditions, the PO₄ uptake in the size fraction > 3 μm correlated with Chl *a* and the P content of phytoplankton.

Relationship between	<i>f</i> CO ₂ (μatm)	Significant responses		
		<i>r</i>	<i>p</i>	<i>n</i>
PP–TP	365	0.599	0.008	18
	368	0.515	0.029	18
PP–Chl <i>a</i>	365	0.479	0.0130	25
	368	0.584	0.0022	25
PO ₄ –Chl <i>a</i>	365	–0.832	<0.0001	21
	368	–0.756	0.0011	20
	497	–0.674	0.0008	21
	821	–0.524	0.0147	21
	1007	–0.634	0.0027	20
PP–PC	365	0.542	0.0061	24
	368	0.625	0.0011	24
	497	0.404	0.0490	24
	821	0.551	0.0052	24
DOP–temperature	1007	0.488	0.0470	17
	1231	0.525	0.0310	17
PO ₄ uptake > 3 μm–Chl <i>a</i>	497	0.743	0.0056	12
	821	0.674	0.0081	14
	1231	0.476	0.0310	14
PO ₄ uptake > 3 μm–POP/Chl <i>a</i>	497	–0.601	0.0380	12
	821	–0.631	0.0160	14
	1231	–0.626	0.0165	14

Table 3. Contribution of different phosphorus components to DOP in the mesocosms and in the fjord.

<i>f</i> CO ₂ (μatm)	Contribution to DOP (%)					
	ATP-P	PL-P	DNA-P	RNA-P	sum	unidentified P
Fjord	0.7	0.7	0.04	69.4	70.84	29.16
365	0.7	0.5	0.03	44.1	45.33	54.67
368	0.6	0.5	0.03	46.9	48.03	51.97
497	0.6	0.4	0.04	49.5	50.54	49.46
821	0.6	0.4	0.03	41.8	42.83	57.17
1003	0.8	0.4	0.04	60.1	61.34	38.66
1231	0.5	0.4	0.03	48.6	49.53	50.47

13, PO₄ declined by 0.06 μmol L^{–1} (or 3.5 nmol L^{–1} day^{–1}) from initial values of 0.16 ± 0.01 μmol L^{–1} (Fig. 5d). Subsequently, concentrations increased again, by an average of 2.6 nmol L^{–1} day^{–1}, until the end of the experiment. There were no significant differences between CO₂ treatments until day 23, when high CO₂ concentrations led to slightly lower PO₄ concentrations (Fig. 5d). Afterwards, PO₄ concentrations in the high *f*CO₂ mesocosms were significantly lower than those in the untreated mesocosms (*t* = 6.51, *p* = 0.0003). This observation is in accordance with the dy-

namics of PP and Chl *a* concentrations, which were significantly elevated in the high CO₂ treatments. Thus, the transformation of PO₄ to POP via stimulated biomass formation may have been promoted under high CO₂ conditions in phase III.

Since PO₄ was never fully exhausted, phosphorus limitation of phyto- and bacterioplankton can be excluded. This interpretation is supported by the PC : PP ratios, which varied between 84.4 and 161.1 in all treatments (Paul et al., 2015b) deviating only slightly from the Redfield ratio.

3.1.4 Uptake of PO₄ and ATP

PO₄ turnover times of 1.5–8.4 days (mean 4.0 ± 1.2 days, *n* = 112) in all mesocosms indicated no dependency on the CO₂ treatment (Fig. 9a). Gross PO₄ uptake rates were in the range of 0.6–3.9 nmol L^{–1} h^{–1} (mean 1.7 ± 0.6 nmol L^{–1} h^{–1}, *n* = 112), or 14.3–94.4 nmol L^{–1} day^{–1} (mean 41.3 ± 13.8 nmol L^{–1} day^{–1}; Fig. 9b, Table 4). The rates were highest on days 4 and 9 (phase I) and decreased thereafter until day 15, followed by an increase to a mean maximum rate of 2.3 ± 0.5 nmol L^{–1} h^{–1} (*n* = 6) at day 27. The size fraction < 3 μm was responsible for 59.1 to

Table 4. PO₄- and ATP uptake rates in the fjord and in the mesocosms. Minimum, maximum and mean values as well as the contribution of the size fraction <3 μm to the total activity are given for the whole period of investigation (each: *n* = 16 for PO₄ and *n* = 6 for ATP uptake).

<i>f</i> CO ₂	Total PO ₄ uptake (n mol l ⁻¹ h ⁻¹)			portion (%) < 3 μm	Total ATP-P uptake (n mol l ⁻¹ h ⁻¹)			portion (%) < 3 μm
	min	max	mean		min	max	mean	
Fjord	0.87	2.81	1.63 ± 0.58	76 ± 15	0.04	0.51	0.26 ± 0.15	92 ± 5
365	0.82	3.89	1.67 ± 0.82	81 ± 11	0.14	1.08	0.43 ± 0.33	96 ± 2
368	0.65	2.74	1.61 ± 0.58	86 ± 7	0.16	0.97	0.47 ± 0.27	96 ± 2
497	0.61	3.03	1.52 ± 0.59	86 ± 6	0.20	1.07	0.54 ± 0.28	96 ± 2
821	0.91	2.83	1.60 ± 0.59	88 ± 8	0.14	0.71	0.36 ± 0.21	97 ± 2
1003	0.67	3.79	1.73 ± 0.85	86 ± 6	0.22	0.69	0.39 ± 0.15	97 ± 1
1231	0.87	2.23	1.53 ± 0.43	87 ± 6	0.17	0.67	0.44 ± 0.17	97 ± 2

98.4 % of the total PO₄ uptake (mean 86.5 ± 7.6 %) whereas the size fraction > 3 μm accounted for only 1.6–40.9 % (mean 13.5 ± 7.4 %). Thus, PO₄ was taken up mainly by picoplankton. However, only the uptake rate by the size fraction > 3 μm was positively related to Chl *a* and inversely related to the P content of the biomass (Table 2). Thus, the PO₄ uptake was obviously stimulated when the phytoplankton biomass increased and the cellular P decreased simultaneously. The relationship between PO₄ uptake by this fraction and Chl *a* became evident only in the CO₂-amended conditions indicating that the interaction between P uptake, cellular P-content and growth of phytoplankton was stimulated under elevated CO₂ conditions.

ATP turnover times of 0.2 to 3.6 days (mean 0.94 ± 0.74 days, *n* = 90) were much shorter than the PO₄ turnover times and did not vary between the treatments (Fig. 9c). Between 0.05 and 0.36 nmol ATP L⁻¹ h⁻¹ (mean 0.14 ± 0.08 nmol L⁻¹ h⁻¹, *n* = 36) were hydrolysed, corresponding to a P supply of 0.14 and 1.08 nmol L⁻¹ h⁻¹ (mean 0.44 ± 0.25 nmol L⁻¹ h⁻¹, *n* = 36). Thus, phosphorus additionally supplied from ATP accounted for ~25 % of that provided by PO₄. The picoplankton size fraction (<3 μm) was responsible for 90–99 % of ATP uptake, with only a marginal portion (1.6–9.5 %) attributable to the phytoplankton fraction > 3 μm (Table 4).

3.2 Hydrography and pool sizes in the fjord

Large variations in *f*CO₂ and pH occurred in fjord water during the period of investigation (Table 1). The relationship of *f*CO₂ with temperature and salinity indicated that the CO₂ conditions were influenced predominantly by changes in the water masses, specifically by upwelling which affected both the relationship of *f*CO₂ with PO₄ and probably the correlation of *f*CO₂ with Chl *a* and PC (Table 2). *f*CO₂ ranged from 207 μatm (Fig. 2a) at days 12–16 when temperatures were highest to 800 μatm at day 33 when deep water input occurred which was indicated by pH below 7.75.

Chl *a* concentrations were between 1.12 and 5.46 μg L⁻¹ (mean 2.29 ± 1.11 μg L⁻¹; *n* = 38), with distinct phases cor-

relating with temperature, salinity and pH. However, the Chl *a* maximum occurred at the beginning of phase II, which was 1–2 days after the maximum temperature. Shortly thereafter, Chl *a* decreased to its lowest level before it increased again, albeit only marginally to 1.93 μg L⁻¹ during phase III (Fig. 4).

TP concentrations from day -3 until day 29 ranged between 0.54 and 0.70 μmol L⁻¹ (mean 0.61 ± 0.04 μmol L⁻¹; *n* = 19; Figs. 5a, 6). With a general decreasing tendency, TP undulated with a frequency of about 10 days in the period of phases 0 to the first half of phase I and of 6 days in the second half of phase I to II. For the period under investigation, the TP fractions had the following characteristics.

PP concentrations varied from 0.13 to 0.30 μmol L⁻¹ (mean 0.20 ± 0.04 μmol L⁻¹; *n* = 29), thus accounting for 23.4–51.8 % (mean 34.7 ± 7.9 %; *n* = 19) of the TP pool. The development of PP over time did not follow that of TP (Fig. 5b). PP concentrations were highest between days 8 and 19, when the accumulation of PP in the biomass was reflected in declining C : P ratios from 180 to 107 (Paul et al., 2015b) and thereafter remained at the low ratio until the end of the measurements. The PP increase in phase III occurred in parallel to Chl *a* and to the PO₄ decrease (Fig. 6). Thus PO₄ was transformed into PP via biomass production. The calculated P content of phytoplankton was 0.05–0.15 (mean 0.1) μmol PP (μg Chl *a*)⁻¹.

DOP substantially contributed (26–45 %) to the TP pool (Fig. 6). Concentrations ranged between 0.19 and 0.29 μmol L⁻¹ (mean 0.24 ± 0.03 μmol L⁻¹; *n* = 17), with high concentrations occurring in parallel to those of TP in phases I and II (Fig. 5c). The very low DOP value of 0.11 μmol L⁻¹, on day 29, was an outlier (Grubbs test). For the whole study period, DOP concentrations correlated positively with PP (*p* = 0.034, *n* = 17) and inversely with PO₄ concentrations (*p* = 0.005, *n* = 17). A similar behaviour between DOP and Chl *a* was restricted to phases 0 and I, whereas the relationship was inverse in phase II (Fig. 8b). As shown in Figure 8a, the DOP and BPP levels alternated with the same rhythm, but inversely, in phases 0 and I and changed to a parallel development in phase II. Statistical analysis was

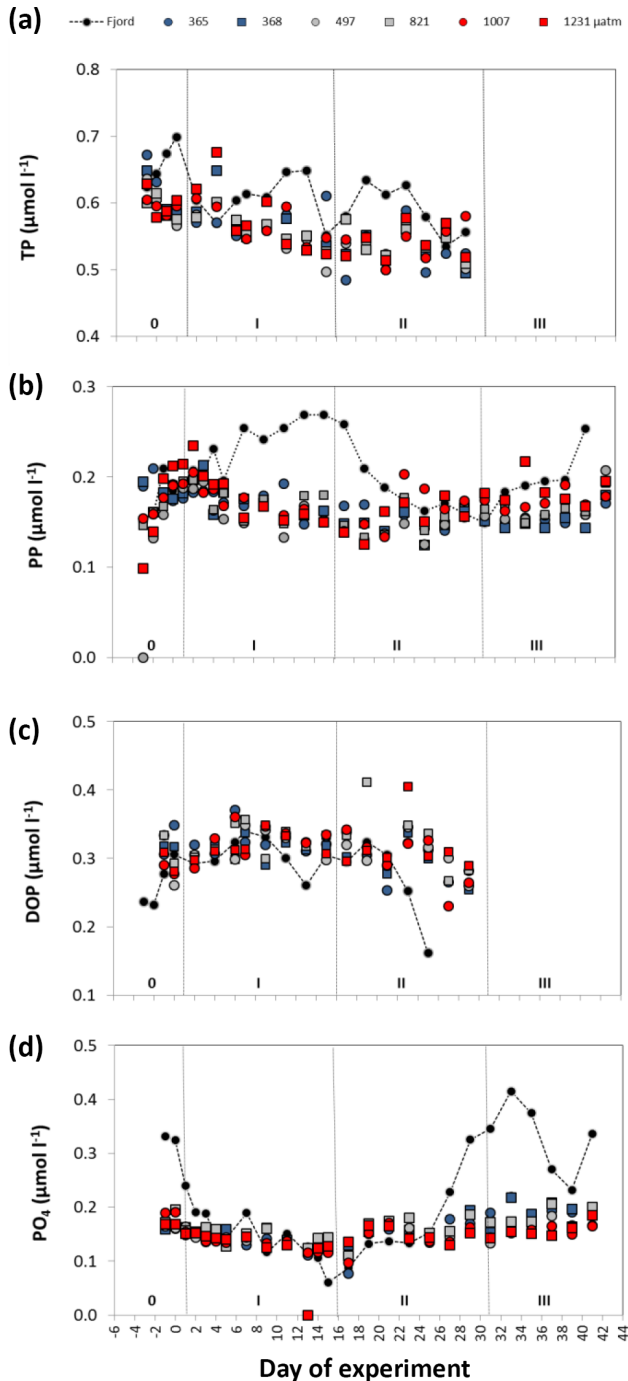


Figure 5. (a–d) Development of total phosphorus (TP) and the three measured P-fractions in fjord water (black dots with dotted line) and in the mesocosms over time. Blue represents untreated, grey intermediate and red high $f\text{CO}_2$ treatment levels.

not feasible because DOP and BPP were not always sampled on the same day and only very few data pairs were available.

PO_4 concentrations ranged between 0.06 and $0.41 \mu\text{mol L}^{-1}$ (mean $0.21 \pm 0.09 \mu\text{mol L}^{-1}$, $n = 21$), thus comprising $24.3 \pm 11.2\%$ ($n = 21$) of the TP pool

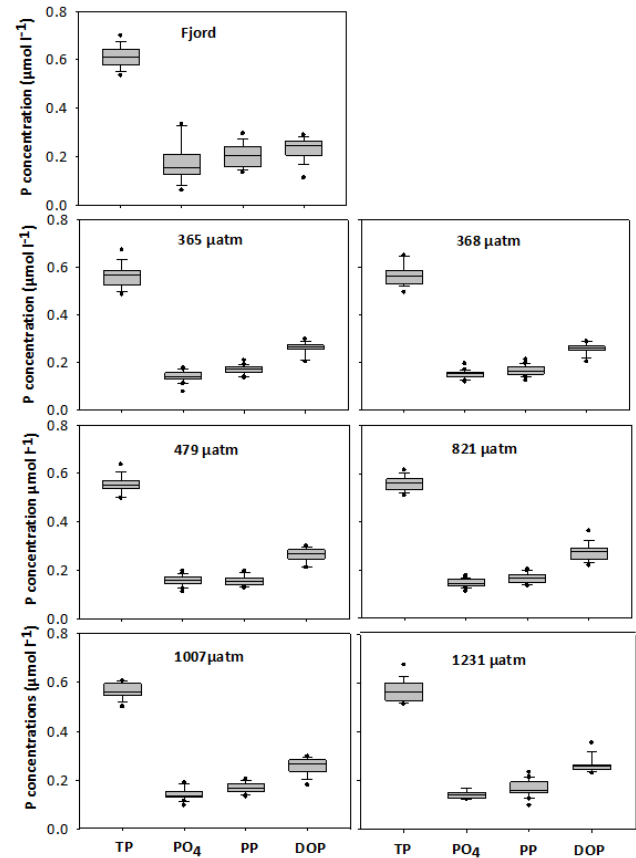


Figure 6. Contribution of the individual P-fractions to TP in fjord water and in the respective mesocosms. The data are averaged for the period when TP measurements were done (day –3 to day 29).

(Fig. 6). With a few exceptions, PO_4 concentrations declined from the beginning of the study period until the end of phase I and increased during phase II and the beginning of phase III. These changes were caused by upwelling of PO_4 enriched deep water of higher salinity and lower temperatures. The subsequent decline in PO_4 between days 33 and 40 was caused by the stimulation of phytoplankton production, as indicated by the increase in Chl *a* concentration (Fig. 4).

4 Discussion

An increase in CO_2 in marine waters and the associated acidification may potentially have multiple effects on organisms and biogeochemical element cycling (Gattuso and Hansson, 2011). Reported findings indicate wide-ranging responses, probably depending on the investigated species and growth conditions. For example, CO_2 stimulation as well as lack of stimulation were found for primary production and carbon fixation (Beardall et al., 2009; Boettjer et al., 2014), DOC release (Engel et al., 2014; MacGilchrist et al., 2014) and phytoplankton growth (Riebesell and Tortell, 2011). An interaction of CO_2 effects with phosphorus and iron avail-

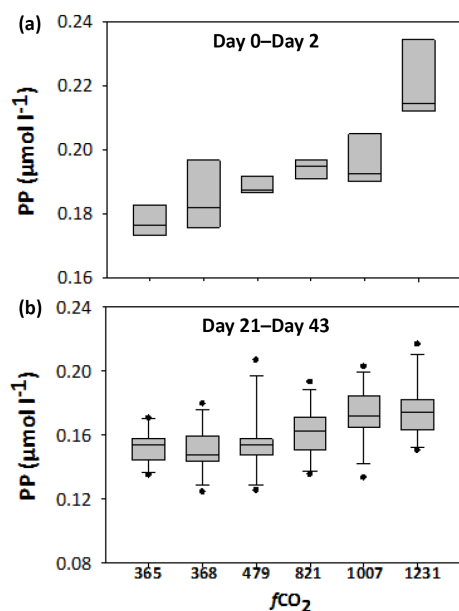


Figure 7. PP concentration in the mesocosms during the initial phase from day 0 to day 2 (a) and from day 23 until the end (b) of experiment.

ability has been found by Sun et al. (2011) for a diatom *Pseudo-nitzschia multiseriata* and by Yoshimura et al. (2014) for a diatom-dominated subarctic plankton community. Thus, responses of organisms and ecosystems to enhanced CO₂ concentrations are complex and still poorly understood. The present study is the first to determine the effects of increased CO₂ levels on phosphorus cycling in a brackish water ecosystem.

4.1 Response of P-pools and P-uptake to enhanced CO₂ in the mesocosms

The Finnish coast off the Gulf of Finland is one of the most important upwelling regions in the Baltic Sea. During our investigation in 2012, surface temperatures, obtained from the NOAA satellite (Siegel and Gerth, 2013), showed that upwelling persisted during the whole study period but with varying intensity. The intensity of upwelling shaped the pattern of temperature not only in the fjord but also in the mesocosms varying from 7.8 to 15.9°C. Such variations in temperature influence the phosphorus transformation and interleave with CO₂ effects.

While nutrients were added in previous CO₂ enrichment experiments (Riebesell et al., 2008, 2013; Schulz et al., 2008), no amendments were undertaken in this study in order to be close to natural conditions. Initial PO₄ concentrations of only $0.17 \pm 0.01 \mu\text{mol L}^{-1}$ were measured, however, PO₄ was never exhausted (Figs. 5, 6). Cellular C:P and N:P ratios were close to the Redfield ratio. Therefore, phosphorus limitation unlikely occurred in this experiment. Simultane-

ous low nitrate and ammonium concentrations (Paul et al., 2015b) formed nutrient conditions that benefit the growth of diazotrophic cyanobacteria. However, a cyanobacteria bloom failed to appear, despite the low-level presence of *Aphanizomenon* sp. and *Dolichospermum* sp. (Paul et al., 2015a) as potential seed stock. For Baltic Sea summer conditions, the phytoplankton development with maximum Chl *a* concentrations of $2.2\text{--}2.5 \mu\text{g L}^{-1}$ remained relatively low with the highest contribution of cryptophytes and chlorophytes in phase I and at the beginning of phase II. Picoplankton was mostly the dominating size fraction, amounting to ~20–70 % of Chl *a* in phase I and up to ~85 % in phase III (Paul et al., 2015b). However, a positive correlation of *f*CO₂ with Chl *a* was observed only for the size fraction >20 µm. The abundance of diatoms that could be a part of this fraction increased from ~day 23 to day 30 and might have an influence on this relationship.

Against this background, the CO₂ perturbation did not cause significant changes in phosphorus pool sizes, DOP composition, and P-uptake rates from PO₄ and ATP when the whole study period was considered. However, small yet significant short-term effects on PO₄ and PP pool sizes were observed in phases I, III and partially in phase II (Fig. 7). CO₂ elevation stimulated the formation of PP until day 3 (Fig. 5b) when chlorophytes, cyanobacteria, prasinophytes and the pico-cyanobacteria started to grow (Paul et al., 2015b).

The effects of CO₂ addition on PO₄ and PP pool sizes were evident from day 23 onwards (Figs. 5b, 7). PO₄ concentrations were slightly, but significantly lower in the high CO₂ treatment than in the untreated mesocosms, accompanied by significantly elevated PP concentrations. This indicates that the transformation of PO₄ into PP was likely stimulated under high CO₂ conditions. Since Chl *a* was also elevated at similar PP:Chl *a* ratios, the PO₄ taken up was used for new biomass formation. However, the elevated transformation of PO₄ into PP was not reflected in the PO₄ uptake rates which can be seen as gross uptake rates. But, an increase of PP, caused by biomass formation, while the PO₄ uptake remained unchanged can only occur when the P release from organisms is reduced. Thus, it is likely the net uptake was modified under CO₂ elevation and not the gross uptake.

While in phases II and III, high CO₂ levels caused a change in the PP and PO₄ pools for about 22 days, changes lasting only 2 days have been observed at the beginning of phase I (Fig. 7a), but, shorter effects cannot be excluded. Uptake and release are assumed to be continuous processes and can alter the P pool sizes on timescales shorter than 1 day. Thus, variations and differences in the treatments can be overseen at daily sampling. Unger et al. (2013) demonstrated that an accelerated PO₄ uptake by the cyanobacterium *Nodularia spumigena* under elevated CO₂ incubations could only be observed during the first hours. Thereafter, the differences were balanced and the same level of radiotracer labelling was reached in all treatments. An acceleration in the formation of particulate P under CO₂ elevation without any

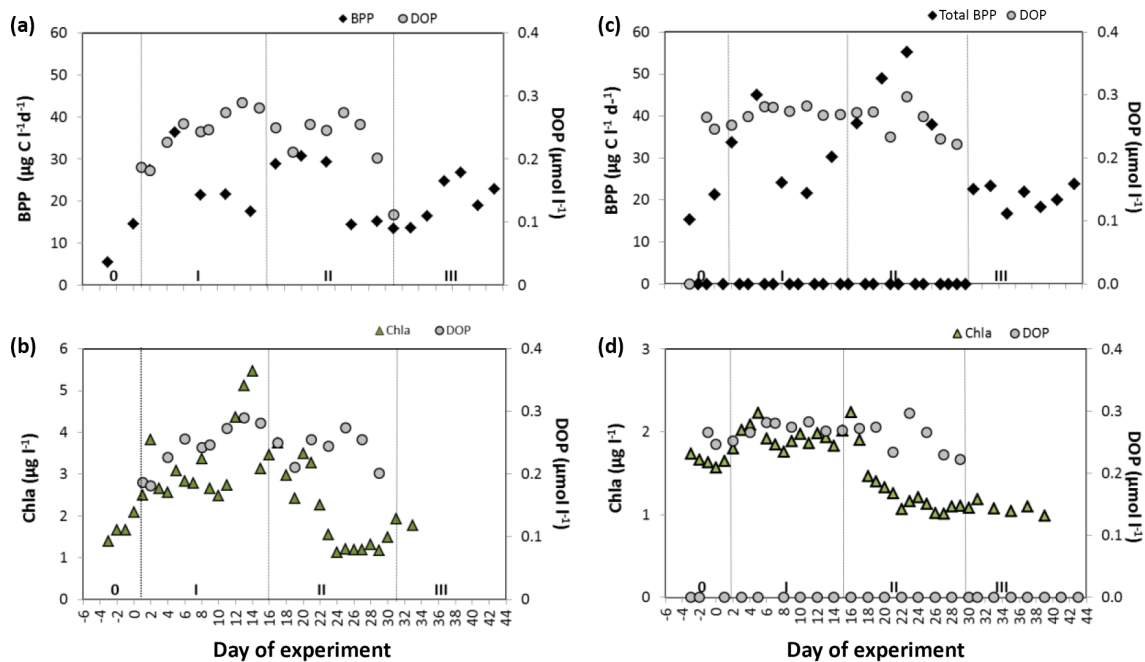


Figure 8. Development of DOP in relation to bacterial production (BPP) and phytoplankton biomass (Chl *a*) in the fjord (a, b) and in the mesocosms (c, d). For mesocosms, mean values averaged over all treatments are given.

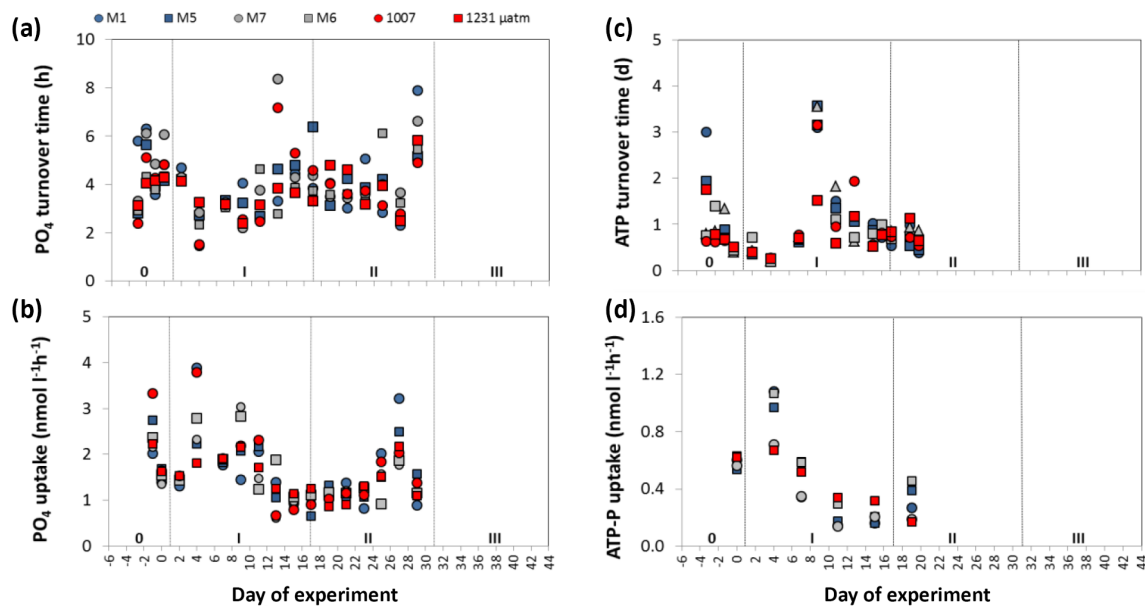


Figure 9. Turnover times of PO₄ (a) and ATP (c) in the mesocosms as well as the respective uptake rates (b, d).

changes of PO₄ turnover times was also observed by Tanaka et al. (2008). They observed an increase of the PP amount and an earlier appearance of the PP maximum under CO₂ elevation.

Correlations calculated by using the Spearman rank test between P pools or uptake rates and other parameters for each mesocosm are presented in Table 2. The relationships

between PP and TP with Chl *a* disappeared at elevated *f*CO₂, whereas correlations developed between PP and PC as well as between the PO₄ uptake by phytoplankton in the >3 µm size class and the PP:Chl *a* ratio (Table 2). These shifts could be caused by changes in the phytoplankton composition deduced from CO₂ effects on the pigment composition (Paul et al., 2015b).

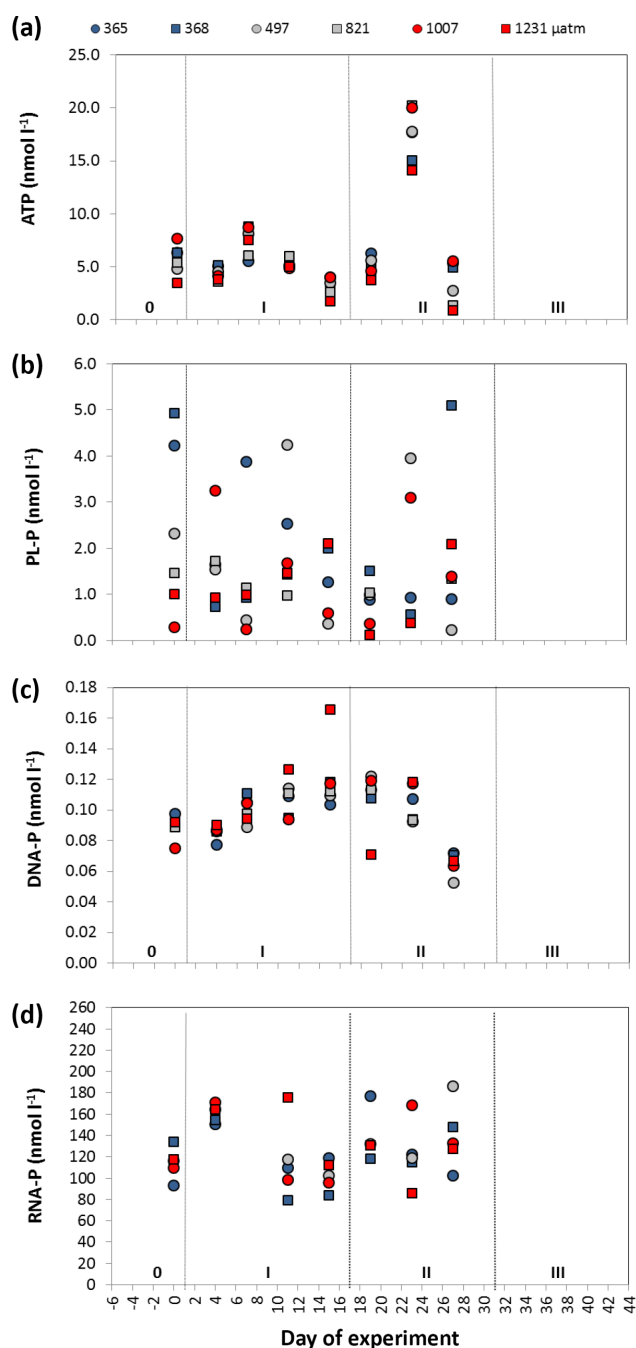


Figure 10. Development of DOP compounds in the mesocosms and in the fjord from day 0 to day 27.

Independent of the CO₂ treatment, TP decreased by $2.6 \text{ nmol L}^{-1} \text{ day}^{-1}$ in all mesocosms over the course of the experiment, in agreement with the measured sedimentation rates (Paul et al., 2015b). The strongest decrease ($\sim 3.2 \text{ nmol L}^{-1} \text{ day}^{-1}$) occurred during phase I. Of the total TP removal during this phase (48 nmol L^{-1}), 84% ($\sim 40.5 \text{ nmol L}^{-1}$) could be explained by the decrease in PP and 16% ($\sim 8 \text{ nmol L}^{-1}$) by changes in the dissolved pool.

However, the PO₄ decline ($\sim 34.5 \text{ nmol L}^{-1}$) was stronger than that of the total dissolved P pool since DOP increased in parallel by $\sim 26.5 \text{ nmol L}^{-1}$. Thus, about 77% of the PO₄ reduction was retrieved as DOP and remained in the dissolved P-pool as the main pathway of PO₄ transformation.

4.2 Phosphorus dynamics in the Storfjärden

Nutrients in upwelled water during our study were depleted in dissolved inorganic nitrogen and enriched in PO₄, as reported for other upwelling areas of the Baltic Sea (Lass et al., 2010). Thus, ammonium and NO₂+NO₃ concentrations in the surface water were only in the nanomolar range (Paul et al., 2015b). PO₄ increased in parallel with the increase in salinity and decrease in temperature. Maximum PO₄ concentrations of 0.33 and $0.42 \mu\text{mol L}^{-1}$ (Figs. 5, 6) were observed at the end of the upwelling events in phases 0 and II, respectively. The correlation with Chl *a* and PP indicated that PO₄ was utilized during plankton growth in the subsequent relaxation phases I and III. Due to PO₄ input into surface water, the phytoplankton community was unlikely P-limited indicated by PC:PP ratios of 86–189 (mean 125, $n = 23$; Paul et al., 2015b). However, the PO₄ availability might be not the only reason for the good P-nutritional status of the plankton. It can be deduced from the long PO₄ turnover times in the mesocosms, where external input was excluded, that the P demand of the plankton community might be low. The P content deduced from PP:Chl *a* ratios of 0.05 – $0.15 \mu\text{mol P} (\mu\text{g Chl } a)^{-1}$ was somewhat lower than those observed during an upwelling event along the east coast of Gotland, where ratios between 0.1 and $0.2 \mu\text{mol P} (\mu\text{g Chl } a)^{-1}$ (Nausch et al., 2009) were estimated.

PP concentrations of 0.13 – $0.3 \mu\text{mol L}^{-1}$ were in the range typically observed in the Baltic Proper (Nausch et al., 2009, 2012). However, PP concentrations in the Gulf of Finland may reach higher values, as was the case in the summer of 2008, when the observed PP concentration was $0.35 \pm 0.07 \mu\text{mol L}^{-1}$ (Nausch and Nausch, 2011).

DOP concentration of $0.27 \pm 0.02 \mu\text{mol L}^{-1}$ during our study was similar to that detected in the Gulf of Finland in the summer of 2008 (Nausch and Nausch, 2011). In the Baltic Sea, DOP exhibits vertical gradients with maximum concentrations in the euphotic surface layer and lower than $0.1 \mu\text{mol L}^{-1}$ at depths below 25 m. Thus, the observed DOP dynamics in surface water during our study can be assumed to be the result of release, consumption and mineralization by organisms or input from land. The relationship of DOP with Chl *a* and BPP (Fig. 8) indicated that the increased DOP concentrations in phase I may be due to release by phytoplankton supplemented by bacterial release. DOP can be accumulated in water only when the release exceeded the consumption or degradation. During phase II, phytoplankton biomass was low and DOP release should thus be minor. Since the small mesozooplankton increased in the fjord similar to those reported for the mesocosms in phases II and III (Paul et al.,

2015b) DOP could be released during grazing combined with the observed temporal offset of BPP and DOP maxima. Thus, the observed DOP variations may be the result of processes in the surface water.

5 Conclusions

Surface water in Storfjärden showed highly variable $f\text{CO}_2$ conditions and reached levels of up to 800 μatm , which is similar to that expected in ca. 100 years from now. Deduced from the high frequency of upwelling events, organisms experience elevated $f\text{CO}_2$ more or less regularly. Thus, a general impact of $f\text{CO}_2$ on P pools and P uptake rates in the mesocosms could not be identified for the overall period of investigation. However, short-term responses to $f\text{CO}_2$ elevation lasting only few days were observed for the transformation of PO_4 into PP that was linked with stimulation of phytoplankton growth. Although statistically significant, it is difficult to assess if the differences between the treatments are of ecological relevance. Such short-term variations are possible in the phosphorus dynamics since the pools size can be transformed within hours and there changes are in the nanomolar concentration range. There are also indications that relationships of P pool sizes or uptake with Chl *a* and PC can change as $f\text{CO}_2$ increases, but the underlying mechanisms are still unclear. The transformation of PO_4 into DOP was not affected by CO₂ elevation. It may be the major pathway of phosphorus cycling under hydrographical and phytoplankton growth conditions as occurred in our experiment.

Acknowledgements. We are grateful to the KOSMOS team for their invaluable help with the logistics and maintenance of the mesocosms throughout the experiment. In particular, we sincerely thank Andrea Ludwig for organizing and coordinating the campaign and for the daily CTD measurements. We appreciate the assistance of Jehane Ouriqua in the nutrient analysis and that of many other participants who carried out the samplings. We also appreciate the collegial atmosphere during the work and thank everyone who contributed to it. We would also like to acknowledge the staff of the Tvärminne Zoological Station for their hospitality and support, for allowing us to use the experimental facilities, and for providing CTD data for the summers of 2008–20011. Finally, we thank Jana Woelk for analysing the phosphorus samples in the IOW. This study was funded by the BMBF project BIOACID II (FKZ 03F06550).

Edited by: C. P. D. Brussaard

References

Ammerman, J. W., Hood, R. R., Case, D., and Cotner, J. B.: Phosphorus deficiency in the Atlantic: an emerging paradigm in oceanography, *Eos* (Washington DC), 84, 165–170, 2003.

- Beardall, J., Stojkovic, S., and Larsen, S.: Living in a high CO₂ world: impacts of global climate change on marine phytoplankton, *Plant. Ecol. Divers.*, 2, 191–205, 2009.
- Bellerby, R. G. J., Schulz, K. G., Riebesell, U., Neill, C., Nondal, G., Heegaard, E., Johannessen, T., and Brown, K. R.: Marine ecosystem community carbon and nutrient uptake stoichiometry under varying ocean acidification during the PeECE III experiment, *Biogeosciences*, 5, 1517–1527, doi:10.5194/bg-5-1517-2008, 2008.
- Bhaya, D., Schwarz, R., and Grossman, A. R.: Molecular Response to environmental stress, in: *The Ecology of Cyanobacteria*, edited by: Whitton, B. A. and Potts, M., 397–442, 2000.
- Björkman, K. M. and Karl, D. M.: A novel method for the measurement of dissolved adenosine and guanosine triphosphate in aquatic habitats: applications to marine microbial ecology, *J. Microbiol. Meth.*, 47, 159–167, 2001.
- Boettjer, D., Karl, D. M., Letelier, R. M., Viviani, D. A., and Church, M. J.: Experimental assessment of diazotroph responses to elevated seawater $p\text{CO}_2$ in the North Pacific Subtropical Gyre, *Global Biogeochem. Cy.*, 28, 601–616, 2014.
- Borges, A. V., Delille, B., and Frankignoulle, M.: Budgeting sinks and sources of CO₂ in the coastal ocean: Diversity of ecosystems counts, *Geophys. Res. Lett.*, 32, 1–4, 2005.
- Caldeira, K. and Wickett, M. E.: Ocean model predictions of chemistry changes from carbon dioxide emissions to the atmosphere and ocean, *J. Geophys. Res.-Oceans*, 110, 1–12, 2005.
- Clayton, T. D. and Byrne, R. H.: Spectrophotometric seawater pH measurements: total hydrogen ion concentration scale calibration of m-cresol purple and at-sea results, *Deep-Sea Res. Pt. I*, 40, 2115–2129, 1993.
- Czerny, J., Barcelos e Ramos, J., and Riebesell, U.: Influence of elevated CO₂ concentrations on cell division and nitrogen fixation rates in the bloom-forming cyanobacterium *Nodularia spumigena*, *Biogeosciences*, 6, 1865–1875, doi:10.5194/bg-6-1865-2009, 2009.
- Dickson, A. G., Sabine, C. L., and Christian, J. R.: Guide to best practices for ocean CO₂ measurements, North Pacific Marine Science Organization, (PICES Special Publication, 3) Sidney, BC, Canada, 191 pp., available at: <http://aquaticcommons.org/1443/> (last access: 7 March 2016), 2007.
- Eichner, M., Rost, B., and Kranz, S. A.: Diversity of ocean acidification effects on marine N-2 fixers, *J. Exp. Mar. Biol. Ecol.*, 457, 199–207, 2014.
- Eisler, R.: Ocean Acidification. A comprehensive overview, Science Publisher, St. Helier, Jersey, British Channel Islands, 252 pp., 2012.
- Endres, S., Unger, J., Wannicke, N., Nausch, M., Voss, M., and Engel, A.: Response of *Nodularia spumigena* to $p\text{CO}_2$ – Part 2: Exudation and extracellular enzyme activities, *Biogeosciences*, 10, 567–582, doi:10.5194/bg-10-567-2013, 2013.
- Engel, A., Piontek, J., Grossart, H. P., Riebesell, U., Schulz, K. G., and Sperling, M.: Impact of CO₂ enrichment on organic matter dynamics during nutrient induced coastal phytoplankton blooms, *J. Plankton Res.*, 36, 641–657, 2014.
- Frommel, A. Y., Schubert, A., Piatkowski, U., and Clemmesen, C.: Egg and early larval stages of Baltic cod, *Gadus morhua*, are robust to high levels of ocean acidification, *Mar. Biol.*, 160, 1825–1834, 2013.

- Gattuso, J. P. and Hansson, L.: Ocean acidification, Oxford University Press, Oxford, 326 pp., 2011.
- Grasshoff, K., Ehrhardt, M., and Kremling, K. (Eds.): Methods of seawater analysis, Verlag Chemie, Weinheim, 419 pp., 1983.
- Grossart, H. P., Allgaier, M., Passow, U., and Riebesell, U.: Testing the effect of CO₂ concentration on the dynamics of marine heterotrophic bacterioplankton, *Limnol. Oceanogr.*, 51, 1–11, 2006.
- Hiebenthal, C., Philipp, E. E. R., Eisenhauer, A., and Wahl, M.: Effects of seawater $p\text{CO}_2$ and temperature on shell growth, shell stability, condition and cellular stress of Western Baltic Sea *Mytilus edulis* (L.) and *Arctica islandica* (L.), *Mar. Biol.*, 160, 2073–2087, 2013.
- IPCC: Climate Change 2001: The Scientific Basis. Third Assessment Report of the Intergovernmental Panel on Climate Change, Cambridge University Press, New York, USA, 82 pp., 2001.
- IPCC: Climate Change 2013: The Physical Science Basis. Working Group I Contribution to the Fifth Assessment Report of the Intergovernmental Panel on Climate Change, Cambridge University Press, New York, USA, 1435 pp., 2013.
- Jeffrey, S. W. and Welschmeyer, N. A.: Spectrophotometric and fluorometric equations in common use in oceanography, in: *Phytoplankton pigments in oceanography*, edited by: Jeffrey, S. W., Mantoura, R. F. C., and Wright, S. W., UNESCO Publishing, Paris, 1997.
- Johnes, P. and Heathwaite, A. L.: A procedure for the simultaneous determination of total nitrogen and total phosphorus in freshwater samples using persulfate microwave digestion, *Water Res.*, 26, 1281–1287, 1992.
- Karl, D. M.: Phosphorus, the staff of life, *Nature*, 406, 31–33, 2000.
- Karl, D. M. and Bailiff, M. D.: The measurements of dissolved nucleotides in aquatic environments, *Limnol. Oceanogr.*, 34, 543–558, 1989.
- Karl, D. M. and Björkman, K. M.: Dynamics of DOP, in: *Biogeochemistry of marine dissolved organic matter*, edited by: Hansell, D. A. and Carlson, C. A., Academic Press, Amsterdam, 2002.
- Lass, H. U., Mohrholz, V., Nausch, G., and Siegel, H.: On phosphate pumping into the surface layer of the eastern Gotland Basin by upwelling, *J. Mar. Syst.*, 80, 71–89, 2010.
- Llebot, C., Spitz, Y. H., Sole, J., and Estrada, M.: The role of inorganic nutrients and dissolved organic phosphorus in the phytoplankton dynamics of a Mediterranean bay A modeling study, *J. Mar. Syst.*, 83, 192–209, 2010.
- Lomas, M. W., Burke, A. L., Lomas, D. A., Bell, D. W., Shen, C., Dyhrman, S. T., and Ammerman, J. W.: Sargasso Sea phosphorus biogeochemistry: an important role for dissolved organic phosphorus (DOP), *Biogeosciences*, 7, 695–710, doi:10.5194/bg-7-695-2010, 2010.
- Lueker, T. J., Dickson, A. G., and Keeling, C. D.: Ocean $p\text{CO}_2$ calculated from dissolved inorganic carbon, alkalinity, and equations for K-1 and K-2: validation based on laboratory measurements of CO₂ in gas and seawater at equilibrium, *Mar. Chem.*, 70, 105–119, 2000.
- MacGilchrist, G. A., Shi, T., Tyrrell, T., Richier, S., Moore, C. M., Dumousseaud, C., and Achterberg, E. P.: Effect of enhanced $p\text{CO}_2$ levels on the production of dissolved organic carbon and transparent exopolymer particles in short-term bioassay experiments, *Biogeosciences*, 11, 3695–3706, doi:10.5194/bg-11-3695-2014, 2014.
- Mehrbach, C., Culbertson, C. H., Hawly, J. E., Pytkowicz, R., and M., D. J.: Measurement of the apparent dissociation constants of carbonic acid in seawater at atmospheric pressure, *Limnol. Oceanogr.*, 18, 897–907, 1973.
- Morris, A. W. and Riley, J. P.: The determination of nitrate in sea water, *Anal. Chim. Acta*, 29, 272–279, 1963.
- Murphy, J. and Riley, J. P.: A modified single solution method for the determination of phosphate in natural waters, *Anal. Chim. Acta*, 27, 31–36, 1962.
- Nausch, M. and Nausch, G.: Dissolved phosphorus in the Baltic Sea – Occurrence and relevance, *J. Mar. Syst.*, 87, 37–46, 2011.
- Nausch, M., Nausch, G., Lass, H. U., Mohrholz, V., Nagel, K., Siegel, H., and Wasmund, N.: Phosphorus input by upwelling in the eastern Gotland Basin (Baltic Sea) in summer and its effects on filamentous cyanobacteria, *Estuar. Coast. Shelf Sci.*, 83, 434–442, 2009.
- Nausch, M., Nausch, G., Mohrholz, V., Siegel, H., and Wasmund, N.: Is growth of filamentous cyanobacteria supported by phosphate uptake below the thermocline?, *Estuar. Coast. Shelf Sci.*, 99, 50–60, 2012.
- Orr, J. C.: Recent and future changes in ocean carbonate chemistry, in: *Ocean Acidification*, edited by: Gattuso, J. P. and Hansson, L., Oxford University Press, New York, 2011.
- Pajusalu, L., Martin, G., and Pollumae, A.: Results of laboratory and field experiments of the direct effect of increasing CO₂ on net primary production of macroalgal species in brackish-water ecosystems, *P. Est. Acad. Sci.*, 62, 148–154, 2013.
- Pansch, C., Nasrolahi, A., Appelhans, Y. S., and Wahl, M.: Impacts of ocean warming and acidification on the larval development of the barnacle *Amphibalanus improvisus*, *J. Exp. Mar. Biol. Ecol.*, 420, 48–55, 2012.
- Patey, M. D., Rijkenberg, M. J. A., Statham, P. J., Stinchcombe, M. C., Achterberg, E. P., and Mowlem, M.: Determination of nitrate and phosphate in seawater at nanomolar concentrations, *Trac-Trends, Anal. Chem.*, 27, 169–182, 2008.
- Paul, A., Achterberg, E., Ouriqua, J., Bach, L., Schulz, K., Boxhammer, T., Czerny, J., Trense, Y., and Riebesell, U.: No measurable effect of ocean acidification on nitrogen biogeochemistry in a summer Baltic Sea plankton community, *Biogeosciences Discuss.*, 12, 17543–17593, doi:10.5194/bgd-12-17543-2015, 2015a.
- Paul, A. J., Bach, L. T., Schulz, K.-G., Boxhammer, T., Czerny, J., Achterberg, E. P., Hellemann, D., Trense, Y., Nausch, M., Sswat, M., and Riebesell, U.: Effect of elevated CO₂ on organic matter pools and fluxes in a summer Baltic Sea plankton community, *Biogeosciences*, 12, 6181–6203, doi:10.5194/bg-12-6181-2015, 2015b.
- Riebesell, U. and Tortell, P.: Effects of ocean acidification on pelagic organisms and ecosystems, in: *Ocean acidification*, edited by: Gattuso, J. P. and Hansson, L., Oxford University Press, New York, 2011.
- Riebesell, U., Bellerby, R. G. J., Grossart, H.-P., and Thingstad, F.: Mesocosm CO₂ perturbation studies: from organism to community level, *Biogeosciences*, 5, 1157–1164, doi:10.5194/bg-5-1157-2008, 2008.
- Riebesell, U., Czerny, J., von Bröckel, K., Boxhammer, T., Büdenbender, J., Deckelnick, M., Fischer, M., Hoffmann, D., Krug, S. A., Lentz, U., Ludwig, A., Mücke, R., and Schulz, K. G.: Technical Note: A mobile sea-going mesocosm system – new oppor-

- tunities for ocean change research, *Biogeosciences*, 10, 1835–1847, doi:10.5194/bg-10-1835-2013, 2013.
- Rossoll, D., Sommer, U., and Winder, M.: Community interactions dampen acidification effects in a coastal plankton system, *Mar. Ecol.-Prog. Ser.*, 486, 37–46, 2013.
- Sanudo-Wilhelmy, S. A., Kustka, A. B., Gobler, C. J., Hutchins, D. A., Yang, M., Lwiza, K., Burns, J., Capone, D. G., Raven, J. A., and Carpenter, E. J.: Phosphorus limitation of nitrogen fixation by *Trichodesmium* in the central Atlantic Ocean, *Nature*, 411, 66–69, 2001.
- Schulz, K. G. and Riebesell, U.: Diurnal changes in seawater carbonate chemistry speciation at increasing atmospheric carbon dioxide, *Mar. Biol.*, 160, 1889–1899, 2013.
- Schulz, K. G., Riebesell, U., Bellerby, R. G. J., Biswas, H., Meyerhöfer, M., Müller, M. N., Egge, J. K., Nejstgaard, J. C., Neill, C., Wohlers, J., and Zöllner, E.: Build-up and decline of organic matter during PeECE III, *Biogeosciences*, 5, 707–718, doi:10.5194/bg-5-707-2008, 2008.
- Siegel, H. and Gerth, M.: Sea surface temperature in the Baltic Sea in 2012, in: HELCOM Baltic Sea environment fact sheets, available at: <http://www.helcom.fi/baltic-sea-trends/environment-fact-sheet> (last access: 25 September 2015), 2013.
- Simon, M. and Azam, F.: Protein content and protein synthesis rates of planktonic marine bacteria, *Mar. Ecol.-Prog. Ser.*, 51, 201–213, 1989.
- Simon, M. and Rosenstock, B.: Carbon and nitrogen sources of planktonic bacteria in Lake Constance studied by the composition and isotope dilution of intracellular amino acids, *Limnol. Oceanogr.*, 37, 1496–1511, 1992.
- Stemmer, K., Nehrke, G., and Brey, T.: Elevated CO₂ Levels do not Affect the Shell Structure of the Bivalve *Arctica islandica* from the Western Baltic, *PLoS ONE*, 8, e70106, doi:10.1371/journal.pone.0070106, 2013.
- Sugie, K. and Yoshimura, T.: Effects of pCO₂ and iron on the elemental composition and cell geometry of the marine diatom *Pseudo-nitzschia pseudodelicatissima* (Bacillariophyceae), *J. Phycol.*, 49, 475–488, 2013.
- Sun, J., Hutchins, D. A., Feng, Y. Y., Seubert, E. L., Caron, D. A., and Fu, F. X.: Effects of changing pCO₂ and phosphate availability on domoic acid production and physiology of the marine harmful bloom diatom *Pseudo-nitzschia multiseries*, *Limnol. Oceanogr.*, 56, 829–840, 2011.
- Suzumura, M. and Ingall, E. D.: Concentrations of lipid phosphorus and its abundance in dissolved and particulate organic phosphorus in coastal seawater, *Mar. Chem.*, 75, 141–149, 2001.
- Suzumura, M. and Ingall, E. D.: Distribution and dynamics of various forms of phosphorus in seawater: insight from field observation in the Pacific Ocean and a laboratory experiment, *Deep-Sea Res. Pt. I*, 51, 1113–1130, 2004.
- Tanaka, T., Thingstad, T. F., Løvndal, T., Grossart, H.-P., Larsen, A., Allgaier, M., Meyerhöfer, M., Schulz, K. G., Wohlers, J., Zöllner, E., and Riebesell, U.: Availability of phosphate for phytoplankton and bacteria and of glucose for bacteria at different pCO₂ levels in a mesocosm study, *Biogeosciences*, 5, 669–678, doi:10.5194/bg-5-669-2008, 2008.
- Tyrrell, T.: The relative influences of nitrogen and phosphorus on oceanic primary production, *Nature*, 400, 525–531, 1999.
- Unger, J., Endres, S., Wannicke, N., Engel, A., Voss, M., Nausch, G., and Nausch, M.: Response of *Nodularia spumigena* to pCO₂ – Part 3: Turnover of phosphorus compounds, *Biogeosciences*, 10, 1483–1499, doi:10.5194/bg-10-1483-2013, 2013.
- Vehmaa, A., Brutemark, A., and Engstrom-Ost, J.: Maternal Effects May Act as an Adaptation Mechanism for Copepods Facing pH and Temperature Changes, *PLoS ONE*, 7, e48538, doi:10.1371/journal.pone.0048538, 2012.
- Wannicke, N., Endres, S., Engel, A., Grossart, H.-P., Nausch, M., Unger, J., and Voss, M.: Response of *Nodularia spumigena* to pCO₂ – Part 1: Growth, production and nitrogen cycling, *Biogeosciences*, 9, 2973–2988, doi:10.5194/bg-9-2973-2012, 2012.
- Yoshimura, T., Sugie, K., Endo, H., Suzuki, K., Nishioka, J., and Ono, T.: Organic matter production response to CO₂ increase in open subarctic plankton communities: Comparison of six microcosm experiments under iron-limited and -enriched bloom conditions, *Deep-Sea Res. Pt. I*, 94, 1–14, 2014.